Article

Wearable LIG Flexible Stress Sensor Based on Spider Web Bionic Structure

Hehui Zheng [1], Han Wang [1,*], Kunran Yi [1], Jian Lin [1], An Chen [2], Lingming Chen [2], Zebiao Zou [1], Maolin Liu [1], Yuchen Ji [1], Lingzhi Dong [1] and Zhenpei Lin [1]

1 Guangdong Provincial Key Laboratory of Micro Nano Manufacturing Technology and Equipment, State Key Laboratory of Precision Electronic Manufacturing Technology and Equipment, College of Mechanical and Electrical Engineering, Guangdong University of Technology, Guangzhou 510006, China
2 The Analysis and Test Center, Guangdong University of Technology, Guangzhou 510006, China
* Correspondence: wanghangood@126.com

Abstract: Bionic structures are widely used in scientific research. Through the observation and study of natural biological structure, it is found that spider web structure is composed of many radial silk lines protruding from the center and spiral silk lines surrounding the center. It has high stability and high sensitivity, and is especially suitable for the production of sensors. In this study, a flexible graphene sensor based on a spider web bionic structure is reported. Graphene, with its excellent mechanical properties and high electrical conductivity, is an ideal material for making sensors. In this paper, laser-induced graphene (LIG) is used as a sensing material to make a spider web structure, which is encapsulated onto a polydimethylsiloxane (PDMS) substrate to make a spider web structured graphene flexible strain sensor. The study found that the stress generated by the sensor of the spider web structure in the process of stretching and torsion can be evenly distributed in the spider web structure, which has excellent resonance ability, and the overall structure shows good structural robustness. In the experimental test, it is shown that the flexible stress sensor with spider web structure achieves high sensitivity (GF is 36.8), wide working range (0–35%), low hysteresis (260 ms), high repeatability and stability, and has long-term durability. In addition, the manufacturing process of the whole sensor is simple and convenient, and the manufactured sensor is economical and durable. It shows excellent stability in finger flexion and extension, fist clenching, and arm flexion and extension applications. This shows that the sensor can be widely used in wearable sensing devices and the detection of human biological signals. Finally, it has certain development potential in the practical application of medical health, motion detection, human-computer interaction and other fields.

Keywords: spider web structure; sensor; laser-induced graphene; flexible strain sensor

1. Introduction

In recent years, research on flexible electronic devices has become more and more popular [1,2]. Different from traditional rigid devices, the stretchability, flexibility and light weight of flexible sensor devices give them wearability, thus showing a wide range of application prospects in personal intelligent medical systems, motion monitoring systems, human-computer interaction, and other fields [3–7]. Flexible sensors include Piezoresistive flexible sensors [8,9], capacitive flexible sensors [10,11], piezoelectric flexible sensors [12,13], and their different principles show different characteristics. Piezoresistive flexible sensors are more widely used because of their simple device structure and loose requirements for signal processing circuits [14]. This paper introduces a piezoresistive flexible stress sensor based on a spider web bionic structure. The flexible sensor is mainly made of conductive materials and flexible substrate. As the cornerstone of flexible devices, flexible sensing materials have become a research hotspot. In order to meet the requirements of electrical conductivity and flexibility of flexible sensing materials, carbon black [15,16], nano-carbon

materials [17,18], graphene [19,20], metal nanowires [21,22], nanoparticles [23,24], etc., are widely used as sensing materials. Graphene is widely used in flexible sensors due to its good flexibility, electrical conductivity, mechanical strength, and tunable electronic properties [5,25–27]. In addition, the selection of flexible substrates is equally important. The substrates used to make flexible sensors use flexible polymer materials such as silicon-based elastomers, epoxy resins or rubbers. Due to their excellent flexibility and durability, they are normally used as a support substrate [28–30].

The spider web structure sensor studied in this paper is a flexible stress sensor made of graphene as a sensing element and PDMS as a supporting substrate. The structural design of the graphene sensing element refers to natural bionics. After millions of years of natural evolution, creatures in the nature have acquired superb survival skills and strong environmental adaptability, providing an effective way for technological innovation [31,32]. By studying the structural characteristics of the natural spider web, it is found that the spider web structure is an octagonal network composed of a number of radial silk threads protruding from the center and spiral silk threads surrounding the center. The structure has a wide coverage and is connected end to end, thus having excellent resonance induction ability. When it is used in the structural design of the sensor, no matter where the strain occurs, it will be induced through structural resonance, thus greatly improving the sensitivity and stability of the sensor [33–35].

The graphene material used in the spider web structure sensor is laser-induced graphene (LIG), which is synthesized by CO_2 infrared laser scanning on polyimide (PI). When the laser radiation energy reaches $5 \, J/cm^2$, carbonization will be carried out on the surface of PI film, and a photothermal reaction will be generated on PI, thus producing graphene with many five membered rings and seven membered rings [36–38]. Compared with other methods for preparing graphene, laser induced graphene (LIG) has the advantages of simple operation, low cost and high efficiency, and is widely used in the preparation of graphene materials [39,40]. However, the stability and extensibility of LIG devices directly formed on PI substrates are poor [41,42]. In order to solve this problem, the LIG on the PI substrate will be transferred to PDMS so that the sensor has good stability and tensile flexibility. As graphene has a 3D porous structure, liquid PDMS can effectively penetrate into the graphene pores, so that they can blend with the LIG and they can penetrate each other to obtain LIG/PDMS composites [43]. A graphene strain sensor with flexible characteristics can be prepared by transferring graphene from the PI to the PDMS substrate and packaging. The sensor has the advantages of a simple manufacturing process, low manufacturing cost, good detection effect, and the ability to monitor tensile and bending deformation. It has particularly good stability and repeatability in the range of tiny mechanical bending deformation, and is expected to be used in the fields of robot electronic skin, motion detection, human-computer interaction, etc.

2. Experimental Part

2.1. Fabrication and Morphological Characterization of LIG

After millions of years of evolution, natural organisms are constantly adapting to changes in the natural environment, which provides a reference for our scientific research. As shown in Figure 1a, a spider web is common in nature. It is a network structure composed of several radial silk threads protruding from a center and spiral silk threads surrounding the center. The spider web structure as shown in Figure 1b is displayed in the plane. The principle of a piezoresistive strain sensor is that the sensor will deform under the action of external force, so that the resistance value of the sensing element will change dramatically. The stress and strain can be detected by monitoring the change of the resistance value. In order to better meet the needs of this change, the structural form shown in Figure 1c can be obtained through structural improvement. The structure is designed to be circular and the thickness of the sensing element is thickened. This not only ensures good conductivity and stability, but also retains the sensitivity of spider web structure sensing, which determines the structure model for the fabrication of a flexible

strain sensor. In order to effectively produce graphene on PI substrate, we first used a 3D printer (Changlian, Guangzhou, China) to manufacture a volume of $50 \times 50 \times 10$ mm^3 nylon mould. Commercial Capton tape (PI) of 80 μm thickness was cut into 50×50 mm^2, attached to a nylon mold, and placed under a CO_2 infrared laser engraving machine (4040-40W, Baihui, Beijing, China). Set the laser power to 5w and scanning speed to 200 mm/s. LIG can be synthesized on PI by direct scanning of CO_2 infrared laser with wavelength of 10.6 μm. A laser engraver combined with a drawing software can carve a spiderweb pattern of graphene on the PI.
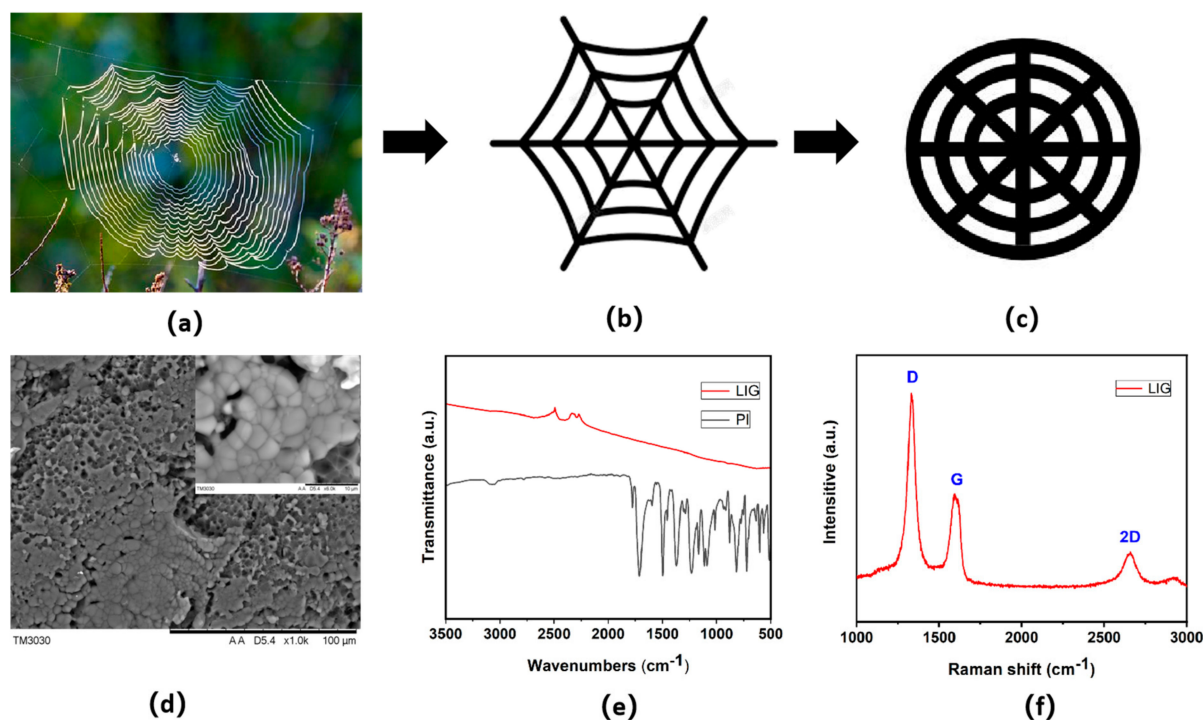
**Figure 1.** (**a**) Natural spider web; (**b**) Spider web planar structure; (**c**) Improved spider web structure; (**d**) SEM microscopy of the structure at 100 μm and 10 μm; (**e**) IR spectra of LIG with PI; (**f**) Raman spectra of LIG.

The prepared LIG/PI samples were characterized. The shape of LIG can be observed by using a scanning electron microscope (SEM, TM3030, Hitachi, Japan). When the LIG is enlarged to 100 μm in the SEM, the planar porous foam structure of graphene can be clearly seen, as shown in Figure 1d. When enlarged to 10 μm, it can be seen that the graphene flakes show ultra-polycrystalline features, with many five-membered and seven-membered rings in the graphene molecular structure. This indicates the porous structure of graphene, which provides a higher surface area and sensitivity for stress sensing. To further indicate the material properties of LIG, the atomic structure of LIG was characterized using Fourier transform infrared absorption spectrometry (FTIR, Nicolet IS50, Thermo Fisher, Waltham, MA, USA) and Raman spectrometry (633 nm laser, LabRAM HR Evolution, HORIBA Jobin Yvon, Palaiseau, France), respectively. As shown in Figure 1e, a Fourier transform infrared absorption spectrometer was used to analyze the LIG sample, and it was found that the energy bands between 1000 cm^{-1} and 1800 cm^{-1} were indicative peaks of C–O bonds, C–N bonds and C=C bonds. To further investigate the atomic structure of LIG, three very distinct protruding peaks on the Raman spectrum of LIG can be seen in Figure 1f: a D peak at 1330 cm^{-1}, a G peak at 1580 cm^{-1}, and a 2D peak at 2665 cm^{-1}. In this case, the G-peak is formed due to the in-plane vibration of sp^2 carbon atoms, while the D-peak is caused either by defects in the graphene itself or by bent sp^2 carbon bonds (bent graphene layers). According to calculations, the intensity ratio of peak G and peak D is about: IG/ID = 2, which indicates that the LIG sample has a high degree of graphene crystallinity.

2.2. The Production of Sensors

The key to making flexible sensor is to use CO_2 infrared laser engraving machine to scan on PI to form LIG and transfer it to flexible substrate. As shown in Figure 2a, the manufacture process of spider web sensor is as follows: stick PI tape on nylon mold, and directly scan PI with CO_2 infrared laser to obtain LIG.In order to transfer the LIG more effectively, fix the LIG inside the nylon mold to ensure that the LIG sample will not become loose. The prepolymer and cross-linker of PDMS (SYLGARD 184, Midland City, MI, USA) were mixed at a mass ratio of A:B = 10:1 to prepare liquid PDMS, the formulated PDMS was placed in a vacuum drying oven (DZF-6213, Yiheng, Shanghai, China), and the air pressure inside the oven was adjusted to -0.08 MPa at room temperature and left for 10 min to remove air bubbles. The Liquid PDMS with the air bubbles removed was then poured into the mold and placed in a vacuum drying oven and set to 75 °C for drying. After 4 h of static drying, the LIG was fully integrated with the PDMS, and the mold was removed after the Liquid PDMS was cured. At this time, the PDMS has been fully integrated into the three-dimensional gap of the LIG, and the LIG/PDMS complex can be obtained after tearing off the PI film. Finally, copper foil was attached to the ports of the sensors individually, and postfixed with conductive silver paint followed by pouring of PDMS for encapsulation. After drying in a vacuum dryer, a flexible sensor with a spider web structure as shown in Figure 2b,c can be obtained. After the graphene is transferred to PDMS, the thickness of graphene transferred to the PDMS substrate was measured by SEM to be 54.7 μm, as shown in Figure 2d, which can be applied to the production of sensors.
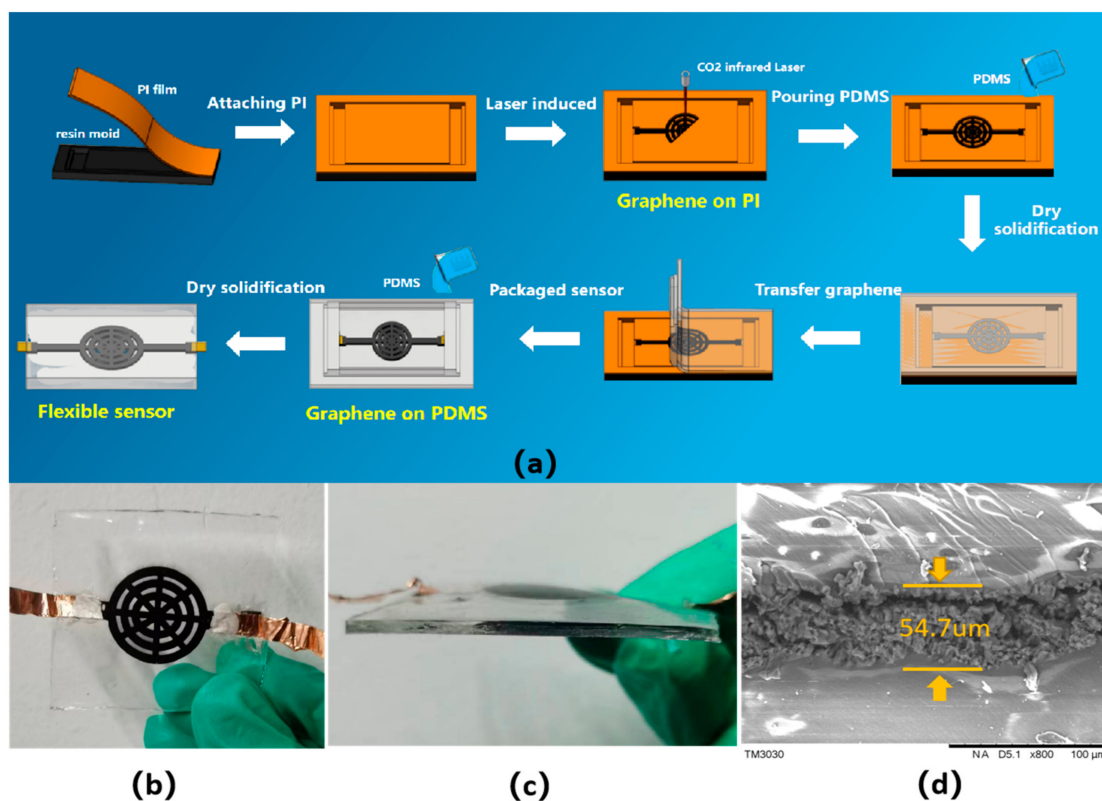
Figure 2. (**a**) Flow chart of the spider web structure flexible sensor fabrication; (**b**) Front view of the spider web structure flexible sensor; (**c**) Side view of the spider web structure flexible sensor; (**d**) Thickness of graphene transferred on the the spider web structure flexible sensor.

3. Results and Discussion

3.1. Steady-State Response Characterization

In order to explore the performance of the spider web structure flexible sensor, the static and dynamic characterization of the sensor is required in the daily experimental envi-

ronment. The sensor is first subjected to tensile experiments to study its static characteristics as well as its dynamic characteristics. The tensile test is performed by mounting the strain transducer on the tensile tester and controlling the different movements of the tensile tester, such as stretching, holding and releasing, by programming the control interface, while monitoring the change of the resistance value of the transducer in real time using an LCR meter (UC2831, UCE, Changzhou, China). To be able to measure the sensor performance well, sensitivity is one of the key performance indicators of flexible sensors and is also based on the characteristic value of linear response. The sensitivity GF of the sensor can be calculated by (1), where R_1 and R_2 represent the resistance values at strain ε_1 and ε_2, respectively, and R_o is the initial resistance value.

$$GF = \frac{(R_1 - R_2)/R_0}{\varepsilon_1 - \varepsilon_2} \tag{1}$$

In order to show the excellent structure and performance of the spider web structure, the planar-LIG sensors with the same shape and size are compared. As shown in Figure 3a, the flexible stress sensor is clamped at both ends of the tension tester and stretched up uniformly at a speed of 100 mm/s. During the stretching process, the data acquisition of resistance changes is carried out by combining the LCR instruments. In order to prevent overload, the strain range of tension shall be controlled within 75%. The data of sensor resistance change collected by LCR can be substituted into the sensitivity formula to calculate the response change between R/R_0 (Ω) and strain (%), as shown in the image in Figure 3b. It can be seen from the figure that the change in resistance of the sensor is positively correlated with the strain within a certain strain range. The linear range between the change in resistance and the change in strain in the planar-LIG sensors is between 0%–46%, and the stable operation of the sensor can be achieved within this period, but the resistance response of the sensor is small and the sensitivity exhibited is smaller. Compared with the planar structure, the sensor GF of the spider web structure is larger and shows higher sensitivity to the strain generated by external stress. In the strain range of 0%–35%, the change of resistance of the sensor of the spider web structure is positively correlated with the change of stress and shows a stable sensing effect. However, due to the brittle nature of graphene, the cracking of LIG increases in the later stages and the change in the resistance of the sensor changes exponentially with strain, thus losing the linearity and reversibility of the resistive response.


(a)　　　　　　　　　　　　　**(b)**
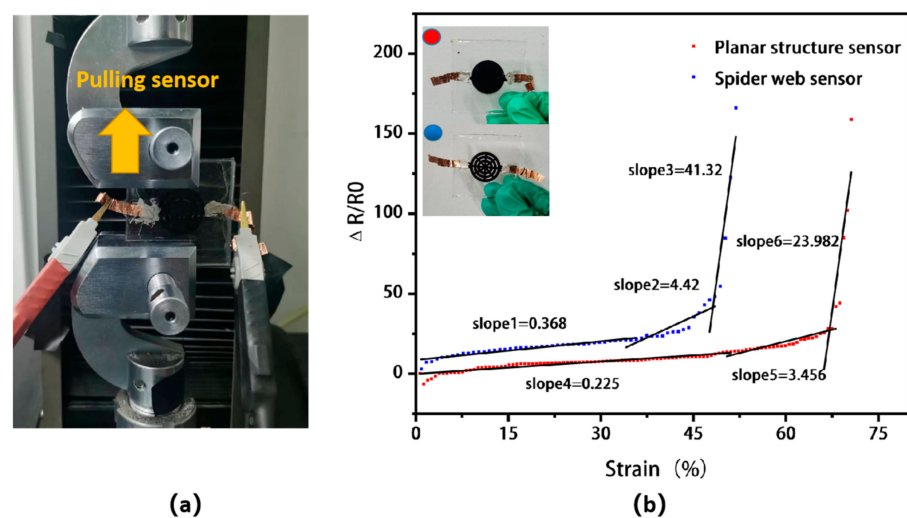
Figure 3. (**a**) Tensile test of spider web sensor and plane sensor; (**b**) Static tensile strain response of the spider web sensor and planar sensor.

3.2. Characterization of Dynamic Response

The above experiments prove the high sensitivity of the spider web structure sensor. Next, experiment and analyze the dynamic response of the spider web structure strain sensor within the linear response range to explore the repeatability, stability, response speed, durability and other performance of the spider web strain sensor. In the above experiments, it was found that the linear response range of the spider web structure sensor is 0–35%. In order to investigate the dynamic performance of the sensor, in this experiment, 10%, 20% and 30% strain loads are set to conduct cyclic tension and release tests on the sensor, respectively. Each group of strain loads is subject to 10 cycles of cyclic tensile release, and the cyclic response as shown in Figure 4a can be obtained by monitoring the resistance change through LCR and reading the data. Figure 4a shows that the signal peaks of each period were similar and no obvious signal distortion and drift phenomenon occurred for the spider web sensor at strain loads of 10%, 20%, 30%, respectively, which indicated the good stability and repeatability of the sensors. To better demonstrate this characteristic, a step response cyclic test was done on the sensor. The spider web sensors were subjected to 8 tensile cycles at 10%, 20%, 30% strain load, respectively. Each cycle was 6 s for 2 s of tensile deformation, 2 s of holding time, and 2 s of relaxation release. Through this cyclic test, it was obtained that the signal of each cycle is very stable, as shown in Figure 4b, without signal distortion, and the sensor has a stable step response under different strain loads, which shows that the spider web structure LIG strain sensor has excellent stability and repeatability. In order to explore the response speed of the sensor, taking a cycle from the step ring test of the sensor can reflect the response/relaxation speed of the sensor, and the response generated under a 10% strain load is shown in Figure 4c. The response time of the spider web structural LIG strain sensor is about 260 ms, and the relaxation time is about 287 ms, which indicates that the response time of the sensor is very fast. To further investigate the stability of the sensor and the effect of dynamic resistance response, the spider web structure sensor was strain loaded with a gradient of 10%, thus obtaining the resistance response of the gradient strain, as shown in Figure 4d, from which it can be concluded that the spider web structure sensor shows a stable response change during the stretching and releasing process. In addition, through the gradient stretching and release of the sensor, a step response of gradient strain as shown in Figure 4e is also obtained. As the strain decreases, the dynamic signal returns to the initial value, showing a dynamic reversible resistance response.

In order to explore the durability of the sensor, under daily temperature and humidity conditions, adjust the tensile tester to 120 mm/min, set a 20% strain load to conduct cyclic lifting, and release it 3000 times. As shown in Figure 5, after 3000 cycles, the signal deviation of the sensor can be kept within 10%, which indicates that the sensor can still maintain a good working state and good durability after being used for a long time.
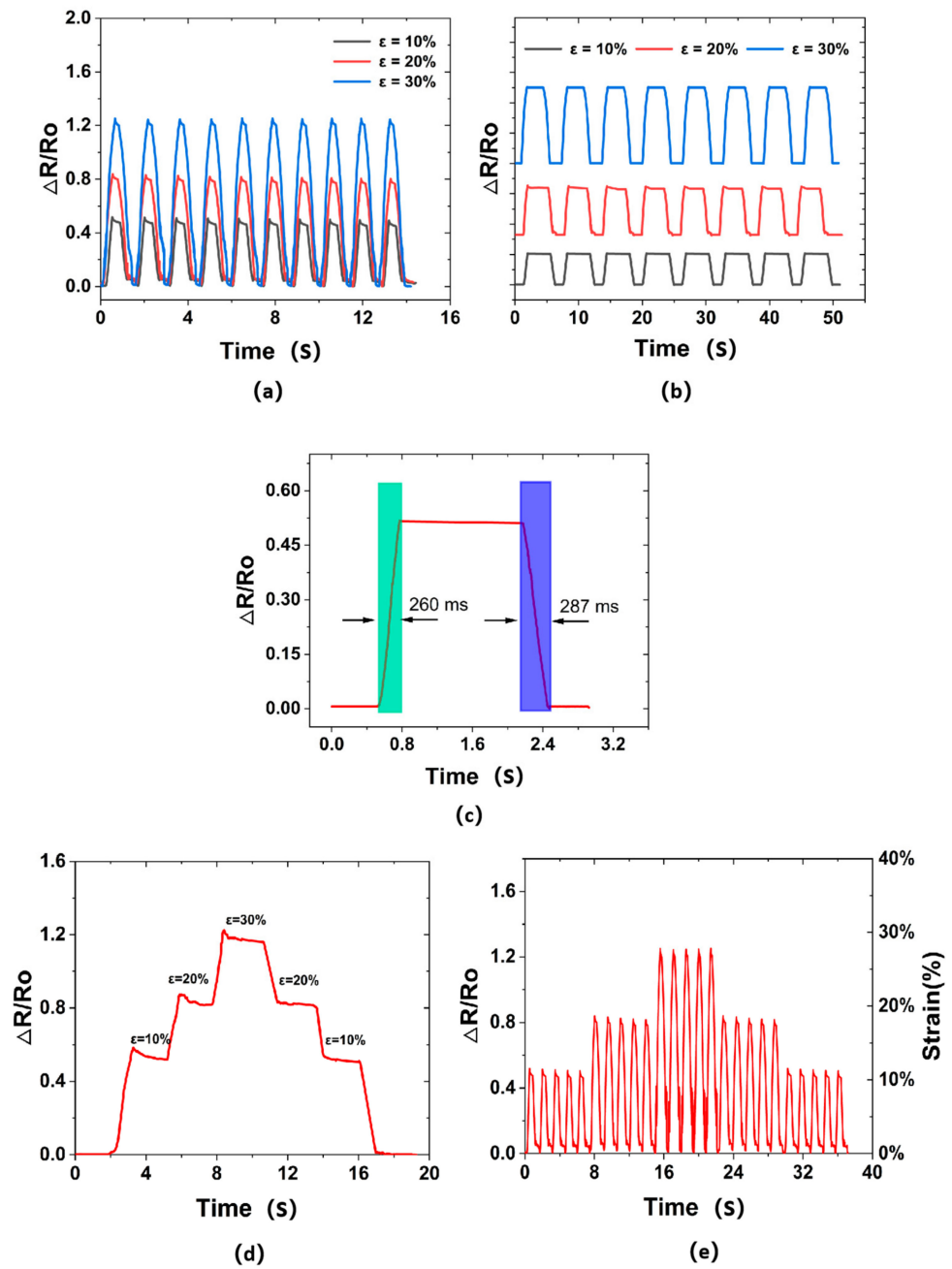
Figure 4. (**a**) Dynamic response of the spider web sensor to 10%–30% strain in the cyclic test; (**b**) step response of the spider web sensor to 10%–30% strain in the cyclic test; (**c**) measurement of the response and relaxation time of the spider web sensor. The response and relaxation times are 260 ms and 287 ms, respectively; (**d**) The step response of the strain varies in a 10% gradient. As the strain decreases, the signal returns to its initial value, showing a dynamic reversible resistive response; (**e**) The dynamic response of the strain varies with a 10% gradient. The resistance variation corresponds to the gradient strain.
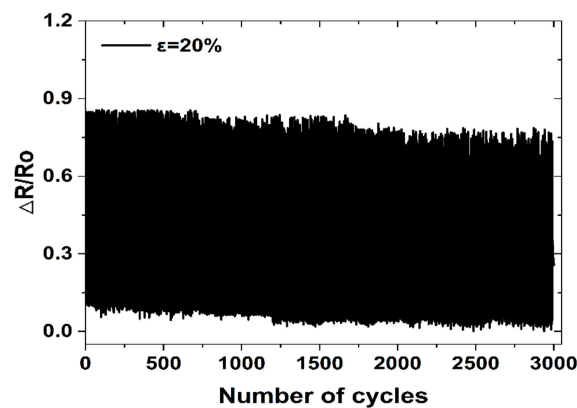
Figure 5. Durability test of the spider web sensor at 20% strain.

4. Application

Due to the outstanding mechanical properties and sensitivity of spider web sensors, the sensors are able to monitor human physiological signals when worn on the skin surface. To show the practical application effect of spider web sensors, finger flexion and extension, clenching one's fist, and arm flexion and extension movements were designed to be detected. The spider web structure sensor is fixed on the finger and detected by LCR circuit connection. When the finger is bent from 0° to 90° and returned to the initial state, the resistance of the spider web sensor changes significantly, and the performance signal as shown in Figure 6a can be obtained after three consecutive finger bends, which are stable and clear and show the process of the finger bending movement. In order to sense the process of making a fist, the spider web structure sensor was fixed on the back of the hand to make a fist movement. Through continuous monitoring by LCR, the resistance signal of the sensor changed significantly. Shown in Figure 6b are the resistance signal changes during the movement of making a fist, to the left of the peak signal is the process of the clenching a fist, which are released after holding for one second. In order to detect the flexion and extension of the arm, fix the cobweb sensor at the elbow joint and swing the arm from 0° to 90° for three cycles. Figure 6c shows that the left side of the peak is the process of arm bending, and the right side of the peak is the process of arm relaxation. The change of resistance signal generated by the sensor can well represent the process of arm flexion and extension. These applications show that the spider web structure sensor provides an important reference for future human motion detection, robot skin and other applications.
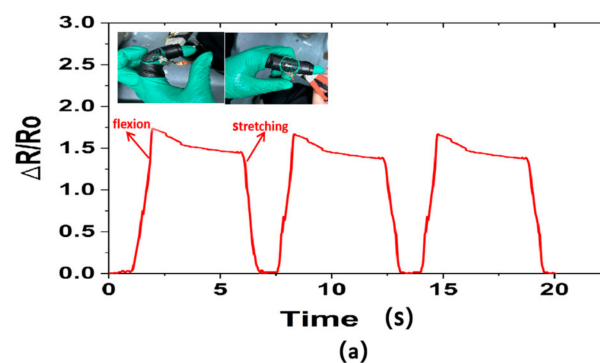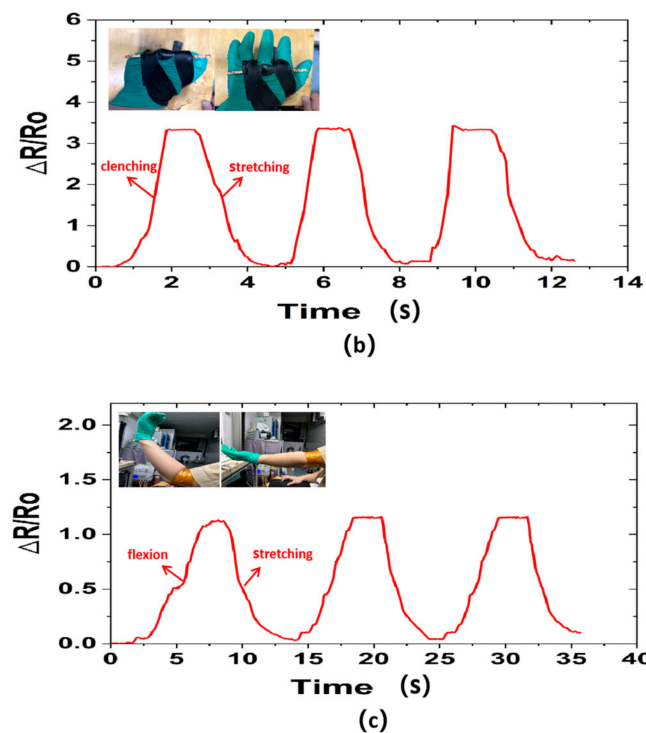

Figure 6. *Cont.*

(b)

(c)

Figure 6. (**a**) flexion and extension of fingers; (**b**) fist clenching and stretching; (**c**) flexion and stretching of the arm.

5. Conclusions

Following the inspiration of natural bionics, in this study we designed and manufactured a new type of graphene flexible stress sensor with reference to a spider web structure. The sensor uses laser induced graphene as a conductive material, combined with a transfer printing process to transfer to a PDMS flexible substrate, and it produces a flexible stress sensor similar to human skin. This method can effectively avoid any physical damage to materials and achieve excellent flexibility. Spider web structure is a network structure extending outward from the center, end to end, covering a wide range, using this structure to make sensors with high sensitivity and good stability. In addition, the manufacturing process of the entire sensor is simple and convenient, and the manufactured sensor is economical and durable. In the experimental characterization, it can be seen that the use range of the cobweb structure sensor is 0%–35%, and the GF under the tensile state reaches 36.8 high sensitivity, of which the response time is about 260 ms, and the relaxation time is about 287 ms. After 3000 cycles of stretching, the sensor is intact and the signal is still stable. These experimental results show that the sensor has high sensitivity, wide working range, low hysteresis, high repeatability, high stability, and long-term durability. These excellent performances predict that flexible sensors of a spider web structure will play an important role in human motion detection, various flexible wearable devices, and robot sensing systems in the future.

Author Contributions: Conceptualization, H.Z. and H.W.; methodology, H.Z.; software, H.Z., Z.L. and J.L.; validation H.Z. and Z.Z.; formal analysis, H.W. and Y.J.; investigation, H.Z. and M.L.; resources, H.Z.; data curation, H.Z. and L.D.; writing—original draft preparation, H.Z.; writing—review and editing, H.W., A.C. and L.C.; visualization, K.Y.; supervision, H.W.; project administration, H.W.; funding acquisition, H.W. All authors have read and agreed to the published version of the manuscript.

References

1. Trung, T.Q.; Lee, N.E. Flexible and stretchable physical sensor integrated platforms for wearable human-activity moni-toringand personal healthcare. *Adv. Mater.* **2016**, *28*, 4338–4372. [CrossRef]
2. Choi, S.; Lee, H.; Ghaffari, R.; Hyeon, T.; Kim, D.-H. Recent advances in flexible and stretchable bio-electronic devices inte-grated with nanomaterials. *Adv. Mater.* **2016**, *28*, 4203–4218. [CrossRef] [PubMed]
3. Wang, C.; Xia, K.; Wang, H.; Liang, X.; Yin, Z.; Zhang, Y. Advanced Carbon for Flexible and Wearable Electronics. *Adv. Mater.* **2018**, *31*, e1801072. [CrossRef]
4. Pang, Z.; Zheng, L.; Tian, J.; Kao-Walter, S.; Dubrova, E.; Chen, Q. Design of a terminal solution for integration of in-home health care devices and services towards the Internet-of-Things. *Enterp. Inf. Syst.* **2013**, *9*, 86–116. [CrossRef]
5. Huang, L.; Wang, H.; Wu, P.; Huang, W.; Gao, W.; Fang, F.; Cai, N.; Chen, R.; Zhu, Z. Wearable Flexible Strain Sensor Based on Three-Dimensional Wavy Laser-Induced Graphene and Silicone Rubber. *Sensors* **2020**, *20*, 4266. [CrossRef] [PubMed]
6. Gao, W.; Emaminejad, S.; Nyein, H.Y.Y.; Challa, S.; Chen, K.; Peck, A.; Fahad, H.M.; Ota, H.; Shiraki, H.; Kiriya, D.; et al. Fully integrated wearable sensor arrays for multiplexed in situ perspiration analysis. *Nature* **2016**, *529*, 509–514. [CrossRef] [PubMed]
7. Park, K.; Tran, P.; Deaton, N.; Desai, J.P. Multi-Walled Carbon Nanotube (MWCNT)/PDMS-Based Flexible Sensor for Medical Applications. In Proceedings of the 2019 International Symposium on Medical Robotics (ISMR), Atlanta, GA, USA, 3–5 April 2019; pp. 1–8.
8. Ma, Y.; Liu, N.; Li, L.; Zou, Z.; Wang, J.; Luo, S.; Gao, Y. A highly flexible and sensitive piezoresistive sensor based on MXene with greatly changed interlayer distances. *Nat. Commun.* **2017**, *8*, 1–8. [CrossRef]
9. Zheng, Q.; Lee, J.-H.; Shen, X.; Chen, X.; Kim, J.-K. Graphene-based wearable piezoresistive physical sensors. *Mater. Today* **2020**, *36*, 158–179. [CrossRef]
10. Yang, J.; Luo, S.; Zhou, X.; Li, J.; Fu, J.; Yang, W.; Wei, D. Flexible, Tunable, and Ultrasensitive Capacitive Pressure Sensor with Microconformal Graphene Electrodes. *ACS Appl. Mater. Interfaces* **2019**, *11*, 14997–15006. [CrossRef]
11. Xiong, Y.; Shen, Y.; Tian, L.; Hu, Y.; Zhu, P.; Sun, R.; Wong, C. A flexible, ultra-highly sensitive and stable capacitive pressure sensor with convex microar-rays for motion and health monitoring. *Nano Energy* **2020**, *70*, 104436. [CrossRef]
12. Hosseini, E.S.; Manjakkal, L.; Shakthivel, D.; Dahiya, R. Glycine–Chitosan-Based Flexible Biodegradable Piezoelectric Pressure Sensor. *ACS Appl. Mater. Interfaces* **2020**, *12*, 9008–9016. [CrossRef] [PubMed]
13. Jung, Y.H.; Hong, K.S.; Wang, H.S.; Han, J.H.; Pham, T.X.; Park, H.; Kim, J.; Kang, S. Flexible piezoelectric acoustic sensors and machine learning for speech processing. *Adv. Mater.* **2020**, *32*, 1904020. [CrossRef] [PubMed]
14. Yang, T.; Xie, D.; Li, Z.; Zhu, H. Recent advances in wearable tactile sensors: Materials, sensing mechanisms, and device performance. *Mater. Sci. Eng. R: Rep.* **2017**, *115*, 1–37. [CrossRef]
15. Ryu, S.; Lee, P.; Chou, J.B.; Xu, R.; Zhao, R.; Hart, A.J.; Kim, S.-G. Extremely Elastic Wearable Carbon Nanotube Fiber Strain Sensor for Monitoring of Human Motion. *ACS Nano* **2015**, *9*, 5929–5936. [CrossRef] [PubMed]
16. Zhu, H.; Wang, X.; Liang, J.; Lv, H.; Tong, H.; Ma, L.; Hu, Y.; Zhu, G.; Zhang, T.; Tie, Z.; et al. Versatile electronic skins for motion detection of joints enabled by aligned few-walled carbon nanotubes in flexible polymer composites. *Adv. Funct. Mater.* **2017**, *27*, 1606604. [CrossRef]
17. Li, C.; Wu, Z.-Y.; Liang, H.-W.; Chen, J.-F.; Yu, S.-H. Ultralight Multifunctional Carbon-Based Aerogels by Combining Graphene Oxide and Bacterial Cellulose. *Small* **2017**, *13*. [CrossRef]
18. Zhang, B.-X.; Hou, Z.-L.; Yan, W.; Zhao, Q.-L.; Zhan, K.-T. Multi-dimensional flexible reduced graphene oxide/polymer sponges for multiple forms of strain sensors. *Carbon* **2017**, *125*, 199–206. [CrossRef]
19. Song, H.; Zhang, J.; Chen, D.; Wang, K.; Niu, S.; Han, Z.; Ren, L. Superfast and high-sensitivity printable strain sensors with bioinspired micron-scale cracks. *Nanoscale* **2016**, *9*, 1166–1173. [CrossRef] [PubMed]
20. Liu, Y.-Q.; Chen, Z.-D.; Mao, J.-W.; Han, D.-D.; Sun, X. Laser Fabrication of Graphene-Based Electronic Skin. *Front. Chem.* **2019**, *7*, 461. [CrossRef]
21. Li, Q.; Ullah, Z.; Li, W.; Guo, Y.; Xu, J.; Wang, R.; Zeng, Q. Wide-Range Strain Sensors Based on Highly Transparent and Supremely Stretchable Graphene/Ag-Nanowires Hybrid Structures. *Small* **2016**, *12*, 5058–5065. [CrossRef]
22. Dong, X.; Wei, Y.; Chen, S.; Lin, Y.; Liu, L.; Li, J. A linear and large-range pressure sensor based on a graphene/silver nanowires nanobiocomposites network and a hierarchical structural sponge. *Compos. Sci. Technol.* **2018**, *155*, 108–116. [CrossRef]
23. Zheng, M.; Li, W.; Xu, M.; Xu, N.; Chen, P.; Han, M.; Xie, B. Strain sensors based on chromium nanoparticle arrays. *Nanoscale* **2013**, *6*, 3930–3933. [CrossRef]

24. Yang, T.; Li, X.; Jiang, X.; Lin, S.; Lao, J.; Shi, J.; Zhen, Z.; Li, Z.; Zhu, H. Structural engineering of gold thin films with channel cracks for ultrasensitive strain sensing. *Mater. Horizons* **2016**, *3*, 248–255. [CrossRef]

25. Yang, H.; Xue, T.; Li, F.; Liu, W.; Song, Y. Graphene: Diversified Flexible 2D Material for Wearable Vital Signs Monitoring. *Adv. Mater. Technol.* **2018**. [CrossRef]

26. Jeong, S.-Y.; Ma, Y.-W.; Lee, J.-U.; Je, G.-J.; Shin, B.-S. Flexible and Highly Sensitive Strain Sensor Based on Laser-Induced Graphene Pattern Fabricated by 355 nm Pulsed Laser. *Sensors* **2019**, *19*, 4867. [CrossRef]

27. Chhetry, A.; Sharifuzzaman, M.; Yoon, H.; Sharma, S.; Xuan, X.; Park, J.Y. MoS2-decorated laser-induced graphene for a highly sensitive, hysteresis-free, and reliable piezoresistive strain sensor. *ACS Appl. Mater. Interfaces* **2019**, *11*, 22531–22542. [CrossRef] [PubMed]

28. Li, X.; Zhang, R.; Yu, W.; Wang, K.; Wei, J.; Wu, D.; Cao, A.; Li, Z.; Cheng, Y.; Zheng, Q.; et al. Stretchable and highly sensitive graphene-on-polymer strain sensors. *Sci. Rep.* **2012**, *2*, 870. [CrossRef]

29. Zhao, Y.; Hu, C.; Song, L.; Wang, L.; Shi, G.; Dai, L.; Qu, L. Functional graphene nanomesh foam. *Energy Environ. Sci.* **2014**, *7*, 1913–1918. [CrossRef]

30. Lv, L.; Zhang, P.; Cheng, H.; Zhao, Y.; Zhang, Z.; Shi, G.; Qu, L. Solution-Processed Ultraelastic and Strong Air-Bubbled Graphene Foams. *Small* **2016**, *12*, 3229–3234. [CrossRef]

31. Han, Z.; Liu, L.; Zhang, J.; Han, Q.; Wang, K.; Song, H.; Wang, Z.; Jiao, Z.; Niu, S.; Ren, L. High-performance flexible strain sensor with bio-inspired crack arrays. *Nanoscale* **2018**, *10*, 15178–15186. [CrossRef]

32. Tian, Q.; Yan, W.; Li, Y.; Ho, D. Bean pod-inspired ultrasensitive and self-healing pressure sensor based on laser-induced graphene and polystyrene microsphere sandwiched structure. *ACS Appl. Mater. Interfaces* **2020**, *12*, 9710–9717. [CrossRef]

33. Ko, F.K.; Jovicic, J. Modeling of Mechanical Properties and Structural Design of Spider Web. *Biomacromolecules* **2004**, *5*, 780–785. [CrossRef]

34. Pugno, N.M.; Cranford, S.W.; Buehler, M.J. Synergetic material and structure optimization yields robust spider web anchor-ages. *Small* **2013**, *9*, 2747–2756. [CrossRef] [PubMed]

35. Su, I.; Qin, Z.; Saraceno, T.; Krell, A.; Mühlethaler, R.; Bisshop, A.; Buehler, M.J. Imaging and analysis of a three-dimensional spider web architecture. *J. R. Soc. Interface* **2018**, *15*, 20180193. [CrossRef] [PubMed]

36. Lin, J.; Peng, Z.; Liu, Y.; Ruiz-Zepeda, F.; Ye, R.; Samuel, E.L.G.; Yacaman, M.J.; Yakobson, B.I.; Tour, J.M. Laser-induced porous graphene films from commercial polymers. *Nat. Commun.* **2014**, *5*, 5714. [CrossRef] [PubMed]

37. Wang, F.; Wang, K.; Zheng, B.; Dong, X.; Mei, X.; Lv, J.; Duan, W.; Wang, W. Laser-induced graphene: Preparation, functionalization and applications. *Mater. Technol.* **2018**, *33*, 340–356. [CrossRef]

38. Ye, R.; James, D.K.; Tour, J.M. Laser-Induced Graphene: From Discovery to Translation. *Adv. Mater.* **2018**, *31*, e1803621. [CrossRef] [PubMed]

39. Nag, A.; Mitra, A.; Mukhopadhyay, S.C. Graphene and its sensor-based applications: A review. *Sens. Actuators A Phys.* **2018**, *270*, 177–194. [CrossRef]

40. Xu, J.; Wang, Y.; Hu, S. Nanocomposites of graphene and graphene oxides: Synthesis, molecular functionalization and applica-tion in electrochemical sensors and biosensors. A review. *Microchim. Acta* **2017**, *184*, 1–44. [CrossRef]

41. Park, J.; Kim, M.; Lee, Y.; Lee, H.S.; Ko, H. Fingertip skin–inspired microstructured ferroelectric skins discriminate static/dynamic pressure and temperature stimuli. *Sci. Adv.* **2015**, *1*, e1500661. [CrossRef]

42. Chen, S.; Jiang, K.; Lou, Z.; Chen, D.; Shen, G. Recent Developments in Graphene-Based Tactile Sensors and E-Skins. *Adv. Mater. Technol.* **2017**, *3*. [CrossRef]

43. Lamberti, A.; Clerici, F.; Fontana, M.; Scaltrito, L. A highly stretchable supercapacitor using laser-induced graphene electrodes onto elastomeric substrate. *Adv. Energy Mater.* **2016**, *6*, 1600050. [CrossRef]